AFRL-AFOSR-JP-TR-2021-0007

Nano-micro-particle and rare earth doped glasses for mid-infrared fiber lasers and microlasers

Ebendorff-Heidepriem, Heike
THE UNIVERSITY OF ADELAIDE
NORTH TERRACE
ADELAIDE, SA, 5005
AUS

08/02/2021
Final Technical Report

Air Force Research Laboratory
Air Force Office of Scientific Research
Asian Office of Aerospace Research and Development
Unit 45002, APO AP 96338-5002

REPORT DOCUMENTATION PAGE

Form Approved
OMB No. 0704-0188

1. REPORT DATE *(DD-MM-YYYY)*	**2. REPORT TYPE**	**3. DATES COVERED** *(From - To)*
02-08-2021	Final	18 Sep 2020 - 17 Mar 2021

4. TITLE AND SUBTITLE
Nano-micro-particle and rare earth doped glasses for mid-infrared fiber lasers and microlasers

5a. CONTRACT NUMBER
FA2386-20-1-4001

5b. GRANT NUMBER

5c. PROGRAM ELEMENT NUMBER

6. AUTHOR(S)
Heike Ebendorff-Heidepriem

5d. PROJECT NUMBER

5e. TASK NUMBER

5f. WORK UNIT NUMBER

7. PERFORMING ORGANIZATION NAME(S) AND ADDRESS(ES)
THE UNIVERSITY OF ADELAIDE
NORTH TERRACE
ADELAIDE, SA 5005
AUS

8. PERFORMING ORGANIZATION REPORT NUMBER

9. SPONSORING/MONITORING AGENCY NAME(S) AND ADDRESS(ES)
AOARD
UNIT 45002
APO AP 96338-5002

10. SPONSOR/MONITOR'S ACRONYM(S)
AFRL/AFOSR IOA

11. SPONSOR/MONITOR'S REPORT NUMBER(S)
AFRL-AFOSR-JP-TR-2021-0007

12. DISTRIBUTION/AVAILABILITY STATEMENT
A Distribution Unlimited: PB Public Release

13. SUPPLEMENTARY NOTES

14. ABSTRACT
See attached

15. SUBJECT TERMS

16. SECURITY CLASSIFICATION OF:			**17. LIMITATION OF ABSTRACT**	**18. NUMBER OF PAGES**	**19a. NAME OF RESPONSIBLE PERSON**
a. REPORT	**b. ABSTRACT**	**c. THIS PAGE**			CHRISTOPHER VERGIEN
U	U	U	SAR	13	**19b. TELEPHONE NUMBER** *(Include area code)* 315-227-7002

Final Report for AOARD Grant FA2386-20-1-4001

"Nano/micro-particle and rare earth doped glasses for mid-infrared fiber lasers and microlasers"

15 June, 2021

Name of first Principal Investigator: Prof Heike Ebendorff-Heidepriem
- e-mail address: heike.ebendorff@adelaide.edu.au
- Institution: The University of Adelaide

Period of Performance: 18 Sep 2020 – 17 Mar 2021

Abstract

This project is closely linked to the Fulbright Scholarship awarded to Prof Ravi Jain (co-PI of this project) at the University of New Mexico to undertake research in the PI Prof Heike Ebendorff-Heidepriem's group in the Institute for Photonics and Advanced Sensing (IPAS) at the University of Adelaide in Nov 2019 - May 2020. The joint objective of this project and the Fulbright Scholarship project is to collaboratively develop advanced glass materials at IPAS (at the University of Adelaide) for novel fiber laser and microlaser applications. The specific aim of this AOARD project (# FA2386-20-1-4001) is the fast-track evaluation of the survival of luminescent ZnSe microcrystals incorporated into "soft" MIR transparent glasses to develop novel class of hybrid materials composed of transition-metal doped semiconductor crystals embedded in glass for broad-band mid-infrared fiber laser and microlaser systems.

The project investigated various low melting point oxide glasses such as lead-silicate, tellurite and sodium germanate and different techniques – such as interface doping and melt doping – for embedding microcrystals in appropriate glasses. ZnSe was selected as the crystal for the initial fast-track evaluation, since transition-metal doped bulk ZnSe crystals have proven to be very attractive mid-infrared laser materials. Undoped semiconductor ZnSe microcrystals show a characteristic "band-edge" blue-green fluorescence, which is helpful to probe the survival of ZnSe in glass. The high refractive index and micron-sized dimensions of the ZnSe crystalllites allowed the use of optical microscopy for identification of the ZnSe microcrystals embedded in glass. Optical and confocal fluorescence microscopy investigations – using 405 nm excitation – of the various samples indicated that ZnSe microcrystals can survive in glass when the doping temperature is at a viscosity of approximately 10^1 dPa·s (honey-like viscosity) or larger. Sodium germanate glasses were found to be an ideal model glass system for studying the embedding of ZnSe in oxide glass, especially since this glass showed minimal background fluorescence at the excitation wavelength of 405 nm of the ZnSe fluorescence. The low background fluorescence allowed observation of fluorescence in the wavelength range of 620-850 nm with peak position up to 740 nm (presumably from defects and/or different environment) in ZnSe particles embedded in germanate glass samples. *The key outcome of this project is advancement in understanding of the physicochemical properties and the suitability of developing hybrid crystal-in-glass composites, laying a solid foundation for future development of hybrid optical glasses for novel broadband laser sources in the visible and mid-infrared spectral ranges.*

1. Introduction

High-beam-quality and high-power mid-IR light sources in the 3-5 μm wavelength range have tremendous potential for a multitude of civilian to military applications, including chemical fingerprint sensing, advanced infrared spectroscopy, medical imaging and diagnostics, time-resolved imaging of molecular structures, and IR countermeasures against heat-seeking missiles. However, the realization of such light sources is technically very challenging [1,2].

Of the various glassy and crystalline materials showing mid-IR fluorescence, Fe^{2+}:ZnSe bulk crystals are exceptional candidates, and have been shown to lase over a broad wavelength range in the 3-5 μm spectral region [3]. However, the difficulty of fabricating crystals in fiber form – which represents an important platform for delivering high-beam-quality high-power laser radiation – has motivated us to incorporate Fe^{2+}:ZnSe crystals into glass hosts [1,2,4], since such glass-based composites may be drawable into optical fibers for eventual power scaling of Fe^{2+}:ZnSe crystallite based MIR laser emission.

The first demonstration of Fe^{2+}:ZnSe-based mid-IR fiber lasers was based on high pressure chemical vapor deposition (HPCVD) to create a Fe^{2+}:ZnSe crystalline region in a silica capillary [4]. Despite its novelty and encouraging optical performance, this fiber concept suffers certain limitations, including low thermal conductivity of the silica outer cladding, short fiber (~1 cm) that can be fabricated, compromised physical integrity of the fiber due to incompatible physical properties, such as thermal expansion coefficient as well as limited optical and mechanical homogeneity. An alternative method is to incorporateFe^{2+}:ZnSe nano-/micro-crystals "extrinsically" into a glass matrix, which is then drawn into fiber. This concept is motivated by the recent advances in successful doping of luminescent nano-/micro-crystals in glass such as upconversion nanoparticles and nitrogen-vacancy containing diamond microcrystals [5,6]. Very recently, early success in doping Fe^{2+}:ZnSe microcrystals into chalcogenide glasses has been demonstrated [2], which strengthens the potential of the multi-phase luminescent composite material concept for the realization of fiber lasers based on Fe^{2+}:ZnSe active luminescent species in passive host glasses. However, chalcogenide glasses exhibit lower mechanical, thermal and crystallization resistance compared to oxide glasses.

Given the long-standing technological maturity in drawing fiber from oxide glasses, this project has focused on identification of a methodology for fast-track evaluation of a suitable oxide glass matrix for embedding Fe^{2+}:ZnSe crystals. Considering the availability of confocal and optical microscopy in the visible spectral range at IPAS, undoped ZnSe microcrystals were selected, which show characteristic semiconductor band-edge emission at ~470 nm upon excitation with available laser at 405 nm. Three glass types were investigated; lead-silicate, tellurite and germanate. The heavy metal oxide free germanate glass system was found to be suitable for embedding ZnSe nano-/micro-crystals as this glass system does not form metallic species during heat-treatment (causing strong background fluorescence) or via reaction with ZnSe (causing disintegration of ZnSe).

2. Glass sample fabrication and appearance

2.1. Selection of glasses and doping techniques

Building on well-researched glass compositions and nano-/micro-crystal doping techniques at IPAS, three glass compositions and two doping techniques were investigated

- Na-Zn-tellurite glass (TZN) [glass fabricated in house]- melt doping
- Na-germanate glass (GN) [glass fabricated in house] - melt doping and interface doping
- commercial (Schott Glass Co) lead-silicate glass (F2) - interface doping

2.2. Preparation of ZnSe micron-size particle suspension for doping

The commercially acquired ZnSe particles in the form of microcrystals had a particle size of approximately 1-5 μm. For melt doping, the particles were used as dry powder. For interface doping and deposition on a glass slide, the particles were first dispersed in ethanol at a concentration about of ~1.2 mg/mL using a magnetic stirrer. Prior to any subsequent use, the suspension was sonicated for ~30 min.

2.3 Overview of samples fabricated

Table 1 lists the various glass samples made in this project using different glass viscosity and temperature for doping the ZnSe particles into the samples.

Table 1: Glass samples – and geometries – fabricated in this project

sample number	sample description	estimated doping viscosity (dPa.s)	doping temperature (°C)
#1	melt-doped ZnSe-TZN glass block	~10^0	577
#2	melt-doped ZnSe-GN glass block	~10^1	1050
#3	interface-doped ZnSe-F2 glass fibre	~10^6	670
#4	interface-doped ZnSe-F2 glass sandwich	~10^6	670
#5	interface-doped ZnSe-GN glass sandwich	~10^6	565
#6	interface-doped ZnSe-GN glass sandwich	~10^1	1050

2.4. Fabrication of sample #1 – Melt doping of TZN glass

The TZN glass batch was melted at 745 °C in an electric furnace at ambient atmosphere. The furnace temperature was subsequently reduced to 577 °C, where the glass viscosity was "oil-like". 0.1 g of ZnSe powder was added into the melt and followed by a manual swirl. Upon adding ZnSe powder into the melt, a puff of black smoke was released. The glass melt with ZnSe powder was "dwelled" for 5 min at 577 °C and then cast into a preheated mold. The sample shows many black particles (Fig. 1 left).

2.5. Fabrication of sample #2 – Melt doping of GN glass

The glass batch was melted at 1250 °C in an electric furnace at ambient atmosphere. The furnace temperature was then reduced to 900 °C, but the glass viscosity was determined to be too high for casting and thus for melt doping. As such, the temperature was increased to 1000 °C, but the glass viscosity was still too high for casting. Hence, the temperature was further increased to 1050 °C, where the glass melt showed a "honey-like" viscosity, which is suitable for casting. 0.1 g of ZnSe powder was added into the glass melt, which was then mildly swirled manually, dwelled for 5 min at 1050 °C and was finally cast into a preheated mold. The resulting glass block showed a red coloured region near the top of the cast glass block, which indicated that the ZnSe particles were not well dispersed and remained near the top of the melt (Fig. 1 right).

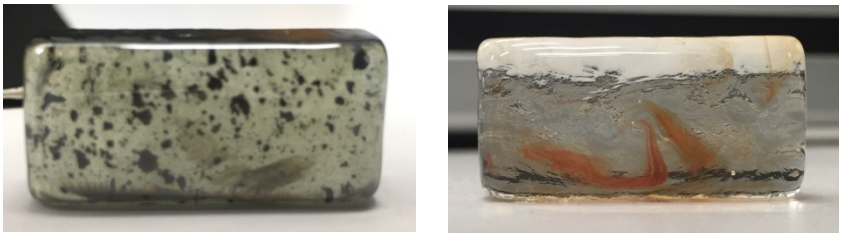

Figure 1: Photographs of melt-doped ZnSe-TZN glass sample #1 (left), and melt-doped ZnSe-GN glass sample #2 (right).

2.6. Fabrication of sample #3 – Interface doping of F2 glass via fiber drawing

An F2 glass rod of ~10 mm diameter and an F2 glass tube of 10 mm outer diameter and ~2 mm inner diameter were fabricated from a commercial glass rod of 30 mm diameter using the billet extrusion technique [7]. The extruded rod of 10 mm diameter was drawn into a thin rod of ~1 mm diameter (hereafter referred to as cane). The cane was dipped in the ZnSe suspension 80 times. This high number of dip coating iterations was employed to achieve a high surface density of ZnSe particles. Note that the ZnSe particles settled relatively quickly from the suspension during the dipping process. Examination of the dip-coated F2 cane with an optical microscope showed the presence of ZnSe particles (with different sizes in μm scale) on the surface of the cane, with most of them in agglomerated and non-uniform distribution (Fig. 2). The ZnSe coated cane was inserted into the F2 tube, and this assembly was drawn in nitrogen atmosphere to a continuous fiber with bands of 250 μm and 160 μm diameter.

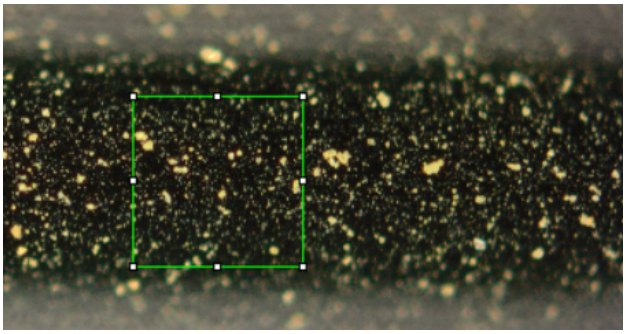

Figure 2: F2 cane dip-coated with ZnSe particles. The green square shows an area of 100 μm × 100 μm with 790 blocks of particles.

2.7. Fabrication of samples #4 and #5 –Interface doping of F2 and GN glass via sandwich sample fabrication simulating fibre drawing conditions

Characterization of the ZnSe doped F2 glass fiber showed that the curved surface hampered the imaging of particles located at the interface. Therefore, the interface doping technique was adapted to plane geometry by making so-called "sandwich" samples, each composed of two slides fused together, with the ZnSe microparticle at the interface between the two slides. To simulate the fiber drawing conditions of interface doping, the slides were heated in a controlled atmosphere furnace under nitrogen flow at a temperature similar to the temperature the glass experienced in the hot zone during fiber drawing. For the F2 glass, mathematical modelling and known temperature-viscosity behavior was used to determine the viscosity (10^6 dPa.s) and glass temperature (670 °C) during drawing [8]. For the GN glass, the temperature-viscosity behavior is unknown. To determine the glass temperature that corresponds to the viscosity of GN glass during fiber drawing, we used the degree of bending of a glass slide at elevated temperature as a measure of viscosity. Specifically, the degree of bending of GN slides at various temperatures was compared to the degree of bending of an F2 slide heated at a temperature (670 °C) corresponding to the glass viscosity during fiber drawing. For these bending tests, a furnace was used where the thermocouple controlling the furnace is situated in the hot zone of the furnace. Thus, the furnace temperature is approximately equal to the glass temperature for a sample in the hot zone. Heat treating GN glass slides at various temperatures revealed that 565 °C resulted in approximately the same GN glass viscosity as the F2 glass viscosity during fibre drawing.

The ZnSe doped F2 and GN sandwich samples were prepared as follows. First, planar F2 and GN slides of ~2 mm thickness were prepared from commercial F2 glass rod and in-house made undoped GN glass block, respectively. A drop of ZnSe suspension (80 μL) was deposited on a slide, and after drying in air, another slide of the same glass was placed on top of the coated slide. This pair of slides with ZnSe particles at slides' interface was placed on a ceramics substrate and then heated at the relevant temperature (670 °C for F2, 565 °C for GN) for 6 minutes in nitrogen atmosphere.

2.8. Fabrication of sample #6 – Interface doping of GN glass via sandwich sample fabrication using glass melting temperature

To compare melt and interface doping, an interface-doped GN sandwich was prepared using the same conditions as for melt doping. This involved placing a part of the ZnSe-doped GN sandwich sample (e) made at 565 °C in an alumina crucible and heating at 1050 °C furnace temperature for 6 minutes in ambient atmosphere in the same furnace that was also used to make sample (b). After cooling down to room temperature, the crucible was broken, leaving shattered pieces of the ZnSe-doped GN sandwich-1050 °C sample behind.

3. Glass sample characterization methods

3.1. Optical microscopy

Commercial optical microscope, with dark field and bright field, was used to image particles deposited on slides or cane and particles embedded in glass fiber or glass sandwich samples.

3.2. Confocal fluorescence microscopy

In-house built confocal fluorescence microscope was used to measure the fluorescence of the various samples in micrometer-scale spatial resolution. A 405 nm laser diode was used for excitation. The excitation light was blocked using a 410 nm bandpass filter. The fluorescence was measured in the range of 410-1000 nm. Due to the use of beam splitter that was coated to back-reflect light at ~530 nm, the measured spectra show a dip at 530 nm, which is a measurement artefact.

4. Results and discussion

4.1. Optical microscopy results

Figure 3 shows photographs of the sandwich samples #4-#6 and dark field optical microscope images of samples #3-#6. For the sandwich samples, the interface was inspected by focusing through the top slide onto the interface. For the ZnSe-F2 fiber #3, short pieces of fiber were cleaved of the drawn fiber and the cross-sectional endface was inspected. In addition, the pieces were inspected from the side along the length of the fiber with focus onto the interface. Each one of these inspections revealed the presence of microparticles at the interface (Fig. 3) with similar appearance before heat-treatment (Fig. 2). This demonstrates the survival of the ZnSe particles when embedded into glass heated at a viscosity of ~10^6 dPa.s in nitrogen atmosphere.

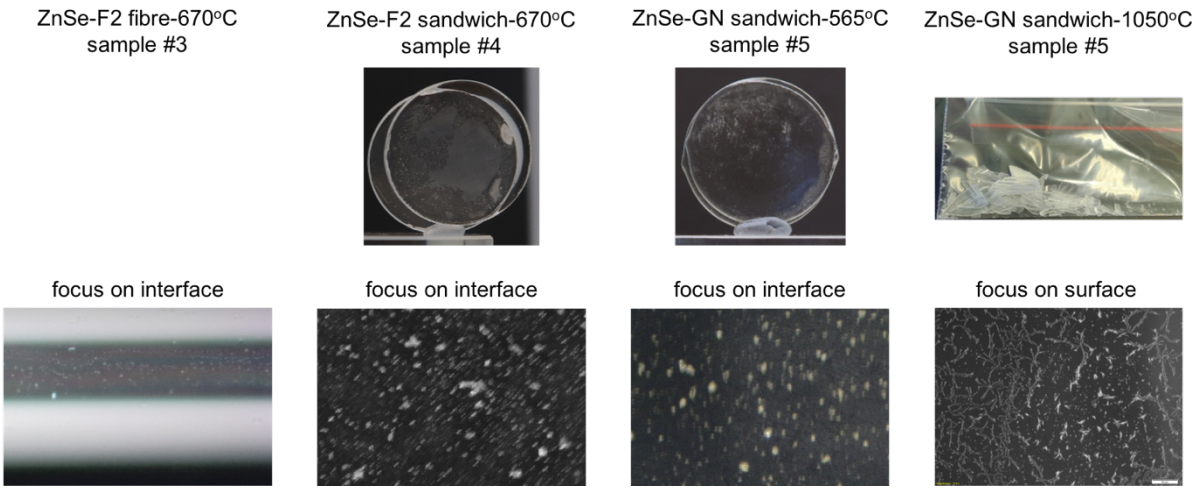

Figure 3: The top row shows photographs of the samples. The bottom row shows optical microscope images taken with 10-20× magnification.

For the ZnSe-GN sandwich-1050 °C sample #6, isolated microparticles and dendrite-like features were found at or close to the surface (Fig. 3 bottom right image). The dendrite-like features are attributed to surface crystallization. The size and morphology of the microparticles suggests that these microparticles were "survived ZnSe particles".

The observation that ZnSe particles are located close to the surface after heat treatment at 1050 °C, while they were located at the interface before heat treatment, is likely caused by pronounced glass flow due the low glass viscosity of 10^1 dPa.s at the 1050 °C heat-treatment.

Before heating, the sandwich sample #5 (565 °C) had a thickness of 3.4 mm, with the interface located in the middle at 1.7 mm from the top. After heating, the sandwich sample #6 (1050 °C) had a thickness of only ~0.6 mm, due to the glass liquid spreading within the ceramic crucible at elevated temperatures. As illustrated schematically in Figure 4, we hypothesize that the glass melting and flowing occurred in a way that the glass above the ZnSe particles moved laterally, bringing the particles closer to the glass surface.

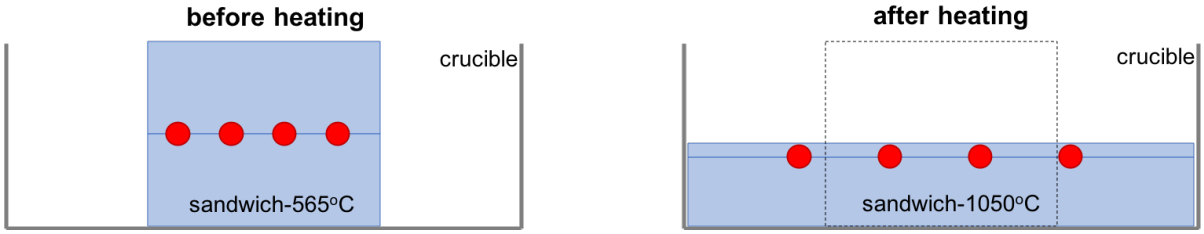

Figure 4: Schematic of ZnSe-sandwich-565 °C sample #5 before heating (left) and after heating (right) at 1050 °C, resulting in the ZnSe-sandwich-1050 °C sample #6. The red circles depict the ZnSe particles.

4.3. Confocal fluorescence microscopy results

ZnSe particles deposited on Si wafer:

The particles show a narrow fluorescence band at 460-480 nm with peak at 470 nm (Fig. 5 right). This band is clearly different than the autofluorescence of the uncoated Si wafer (Fig. 5 left). The 470 nm fluorescence band of the deposited ZnSe microcrystals agrees with the emission of ZnSe bulk crystal at ambient temperature [9].

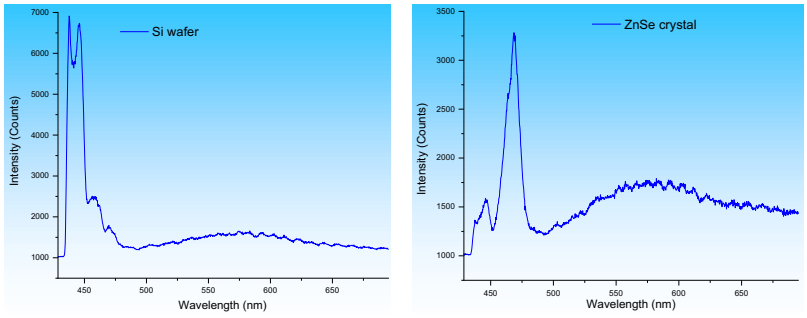

Figure 5: Fluorescence of uncoated Si wafer (left), and ZnSe particles deposited on Si wafer (right).

ZnSe-doped GN samples #2 and #5:

Both the interface doped ZnSe-GN sandwich-565 °C sample #5 made under simulated fiber drawing conditions and the melt doped ZnSe-GN glass sample #2 show similar broad fluorescence band at 620-850 nm with peaks at 720 nm and 740 nm (Fig. 6). This band is significantly broadened and red-shifted compared to ZnSe microparticles deposited on Si wafer (Fig. 5 right). A similar broadened and red-shifted fluorescence at ~560 nm was observed for ZnSe microcrystals grown in borosilicate glass (Pyrex) matrix [9]. This band was ascribed to deep-level emission from crystalline defects or impurities originating from the glass matrix during microcrystal growth. Hence, a possible reason for the broad fluorescence band at

~740 nm in the ZnSe-GN samples #2 and #5 is also the emission of deep-level defect states at the surface of the ZnSe microparticles embedded in glass. We hypothesize that the defects were formed due to reaction of the molten or softened glass with the ZnSe microparticles at the elevated temperature of the doping step. Another explanation of the broadening and red shift of the fluorescence band is the variation of electromagnetic interaction between the crystalline lattice and the host matrix, due in part to index difference, and in part to difference in thermal expansion coefficient (Table 2). In the ZnSe-GN samples #2 and #5, the ZnSe particles are surrounded by high-index GN glass, whereas the deposited ZnSe particles are mostly surrounded by air. The thermal expansion coefficient mismatch between ZnSe and GN might cause stress on the crystal lattice of ZnSe, resulting in a broadening of the emission band. The red-shift of the fluorescence band from ~560 nm in borosilicate glass [9] to ~740 nm in GN glass is consistent with the increase in refractive index from borosilicate glass (1.47) to GN glass (1.64) (Table 2).

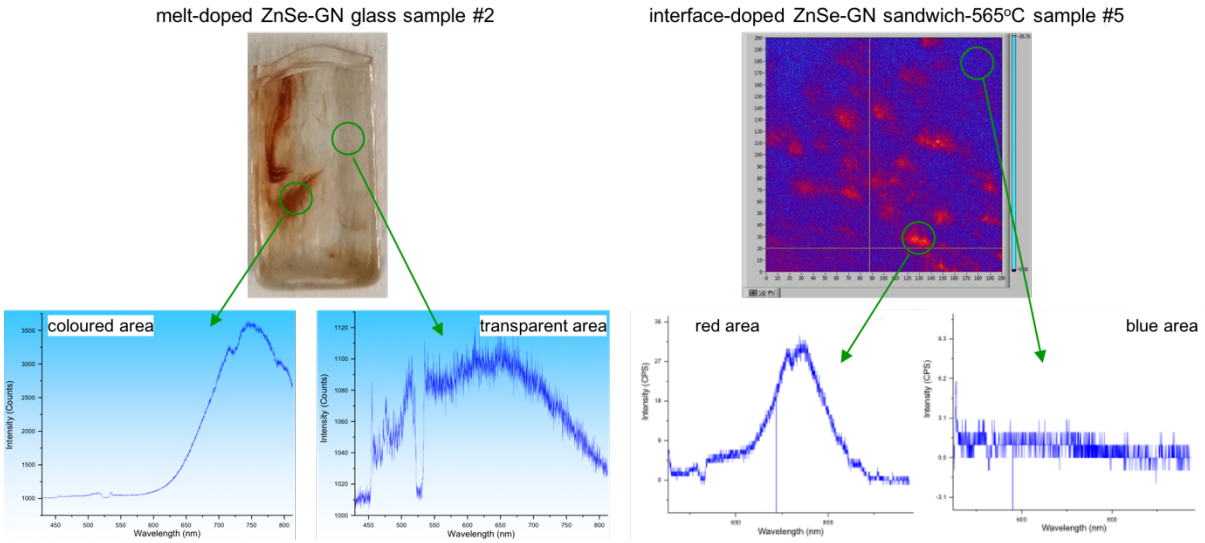

Figure 6: Fluorescence spectra from colored and transparent area of sample #2 (left) and from red and blue area in the confocal image of sample #5 (right).

Table 2: Refractive index of air, F2 glass, GN glass and ZnSe crystal.

	refractive index n_D	thermal expansion coefficient (10^{-6}/K)
air	1.0	n/a
Borosilicate	1.47 [10]	3.3 [10]
F2	1.62 [11]	9.2 [11]
GN	1.64 [12]	9.5 [12]
ZnSe	2.67 [13]	7.4 [14]

ZnSe-doped F2 samples #3 and #4:

For the interface doped ZnSe-F2 sandwich sample #4 made under simulated fiber drawing conditions, the fluorescence spectra collected by focusing on the top and middle of the undoped F2 slide and on the ZnSe-doped interface region show the same broad band at 410-850 nm with peak at ~580 nm (Fig. 7). Considering that F2 and GN glass have similar refractive index and thermal coefficient (Table 2), the ZnSe-F2 sandwich sample is expected to show a similar band with peak at 740 nm as the ZnSe-GN sandwich sample when focusing on the interface region. However, a very broad band with peak at shorter wavelength of ~580 nm is observed, which is also found for the undoped regions. This indicates that the F2 glass shows intense and broad autofluorescence from ~400-850 nm, which obscures any fluorescence in the wavelength range of 650-850 nm from potential defect-containing ZnSe particles. Likewise, for the interface doped ZnSe-F2 fiber sample #3, when scanning across the fiber cross-section as well as inspecting a fiber sample from the side with undertaking a *z*-depth scan from surface to beneath 19 µm with step size 2 µm per scan, only the broad and intense autofluorescence band at ~580nm of the F2 glass itself is found. Since F2 is a lead-silicate glass, we attribute the autofluorescence to the formation of metallic Pb clusters during heating of the F2 glass (irrespective of doping with ZnSe particles). These results demonstrate that F2 glass is not a good candidate for hosting ZnSe particles.

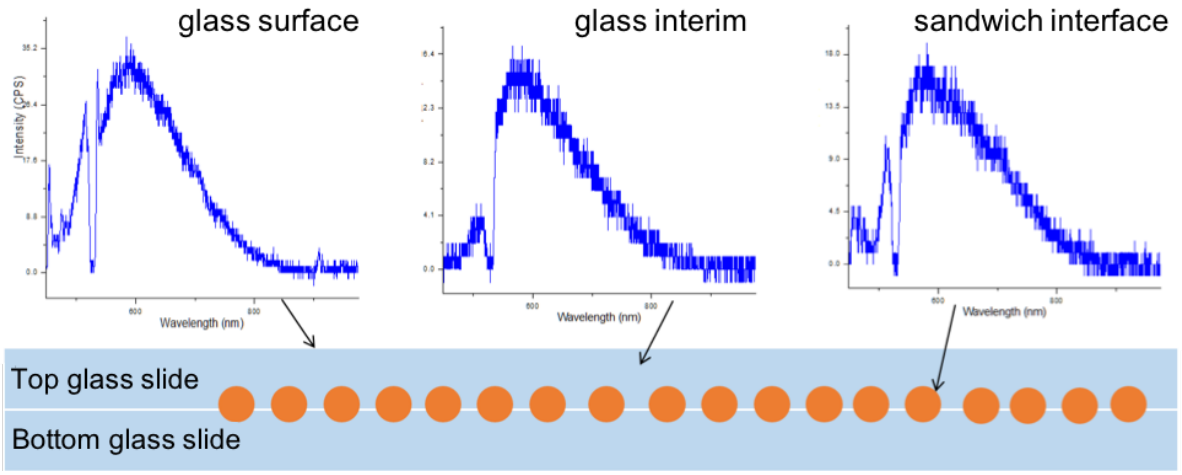

Figure 7: Fluorescence spectra from top surface, interim area and interface of the ZnSe-F2 sandwich sample #4 (top row). Schematic of sandwich sample (with the orange circles depicting the ZnSe particles) and the focal points for the respective fluorescence spectra.

ZnSe-doped TZN sample #1:

The black areas in the melt doped ZnSe-TZN glass #1 show a broad fluorescence band at ~500-800 nm with peak at ~600 nm (Fig. 8 left). In comparison, the red colored areas in the melt doped ZnSe-GN glass #2 show a broad fluorescence band at 620-850 nm with peaks at 720 nm and 740 nm (Fig. 8 right). The difference in color and fluorescence band position and width indicates that the black areas in ZnSe-TZN glass are not from ZnSe particles. The width and position of the band resembles that of metallic tellurium in TZN sol-gel samples [15] and the color resembles that of TZN glass melted under reducing conditions in nitrogen, indicating that the doping of the TZN melt with ZnSe particles led to the formation at metallic tellurium. The

formation of black smoke when adding the ZnSe particles to the hot TZN glass melt is attributed to the formation of selenium vapor considering the low boiling point of 685 °C for elemental selenium. These observations suggest the following chemical redox reaction between the ZnSe particles and the hot TZN glass melt:

$$TeO_2 + 2\ ZnSe \rightarrow Te^0\ \text{(black area in glass)} + 2\ Se^0\ \text{(black vapor)} + 2\ ZnO$$

The vigorous reaction shows that TZN is not a suitable glass host material for doping particles with strong reduction potential due to the easy transformation of Te^{4+} ions in the glass to metallic tellurium.

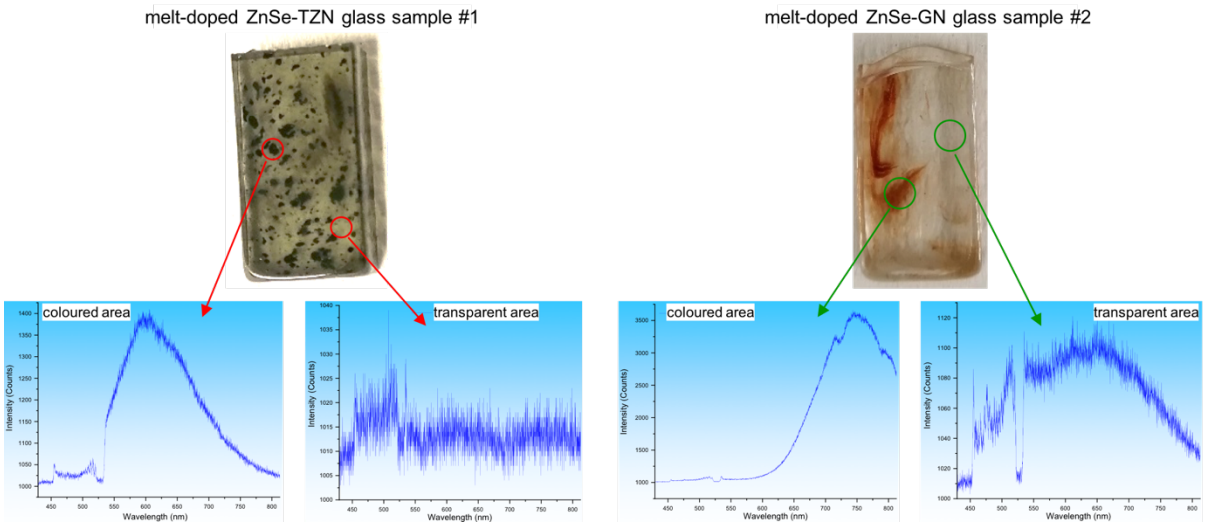

Figure 8: Fluorescence spectra from colored and transparent area of melt doped samples ZnSe-TZN glass #1 (left) and ZnSe-GN glass #2 (right).

ZnSe-doped GN sandwich sample #6:

Compared to the broad emission over ~620-850 nm of ZnSe particles embedded in GN glass for melt-doped sample #2 made at 1050 °C and the interface-doped sample #5 made at 565 °C, the interface-doped GN sandwich sample #6 made at 1050 °C gives rise to a sharp peak at 692 nm, whose peak intensity is about one order of magnitude higher compared to the broad band at ~710 nm it sits on. The FWHM of the sharp peak is about 3 nm, which is about 40 times narrower than that of the fluorescence band at 740 nm of the ZnSe particles in the sandwich-565 °C sample #5 from which the sandwich-1050 °C sample #6 is made. *Future investigations are required to determine whether the sharp peak is caused by ZnSe particles or a new species formed during the heat treatment of sample #5.*

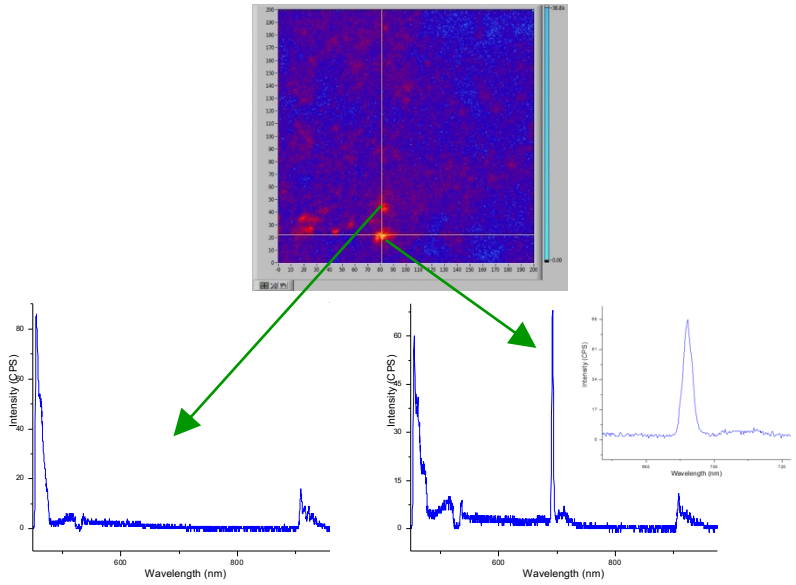

Figure 9: Confocal image of the ZnSe-GN sandwich-1050 °C sample #5 (top) with focus below the sample surface. Fluorescence spectra (bottom) from the respective areas shown by the green arrows. The inset shows the region of the sharp peak at 692 nm.

Conclusions

The embedding of ZnSe microparticles was investigated for three oxide glass types at glass melting and fiber drawing viscosities. For the commercial lead-silicate glass F2, optical microscopy indicates the survival of the ZnSe particles, but confocal fluorescence spectroscopy could not be used to confirm that the survived particles are ZnSe due to the strong autofluorescence of the F2 glass, which is attributed to the formation of metallic Pb. For the Na-Zn-tellurite glass, the ZnSe particles induced a redox reaction between ZnSe and glass matrix, resulting in the disintegration of the ZnSe particles and the formation of metallic Te. These results suggest that heavy metal oxide containing glasses such as lead-silicate and tellurite are not suitable host glasses for the embedding of ZnSe particles due to the tendency of the heavy metal oxides in these glasses to form metallic species at elevated temperature.

Sodium-germanate glass was found to be a suitable host matrix for embedding ZnSe particles at viscosities of glass melting and fibre drawing (~10^1 and ~10^6 dPa.s, respectively). The survival of the ZnSe particles at these viscosities was demonstrated through optical and confocal microscopy. The sodium-germanate glass does not contain heavy metal oxide, preventing autofluorescence and reaction of ZnSe with the glass melt. This behavior suggests that heavy metal oxide free glass is best suited for embedding ZnSe particles into glass.

Suggestions for future work

Three directions are suggested for future work; (i) use of additional characterization technique to confirm the survival of ZnSe particles, (ii) investigation of heavy metal oxide free germanate glass suitable for fabrication of mid-infrared transparent fiber as host matrix, and (iii) exploring fabrication methods that allow high ZnSe doping concentrations with homogeneous distribution of the particles and absence of disintegration of the particles.

X-ray diffraction (XRD) is a widely used technique to identify crystal phases in glass. The challenge of this technique is that only crystal phases with >5-10% volume content can be detected on top of the broad XRD peak caused by the glass matrix itself. Preliminary investigation of the ZnSe-doped sodium-germanate glass made using melt doping showed that the ZnSe particle concentration was insufficient for XRD. A possible alternative is the use of micro-XRD technique.

While the heavy metal oxide free germanate glass system is suggested to be a suitable host glass system, the sodium-germanate glass investigated is likely to be unsuitable for low-loss fiber fabrication due to low crystallization stability. Thus, development or selection of a germanate glass composition (without heavy metal oxides such as PbO, Bi_2O_3, TeO_2) with high crystallization stability and transmission in the 3-5 μm wavelength range is required.

ZnSe particles were successfully embedded in glass in spatially confined regions (interface between glass slides, surface layer of glass melt) at viscosities of ~10^1 and ~10^6 dPa.s. These viscosities are too high to allow homogeneous dispersion of ZnSe particles in the volume of the glass to achieve sufficiently high ZnSe particle concentration for lasing. This motivates the exploration of alternative and advanced fabrication techniques of particle embedding in glass to overcome this limitation.

References

[1] S. D. Jackson, R. Jain, “Fiber-based sources of coherent MIR radiation: key advances and future prospects”, Optics Express 28 (21), 30964-31019 (2020)

[2] M. Chazot, C. Arias, M. Kang, C. Blanco, A. Kostogiannes, J. Cook, A. Yadav, V. Rodriguez, F. Adamietz, D. Verreault, “Investigation of ZnSe stability and dissolution behavior in As-S-Se chalcogenide glasses”, Journal of Non-Crystalline Solids 555, 120619 (2021)

[3] V. V. Fedorov, S. B. Mirov, A. Gallian, D. V. Badikov, M. P. Frolov, Y. V. Korostelin, V. I. Kozlovsky, A. I. Landman, Y. P. Podmar'kov, V. A. Akimov, “3.77-5.05-μm tunable solid-state lasers based on Fe^{2+}-doped ZnSe crystals operating at low and room temperatures”, IEEE Journal of Quantum Electronics 42 (9), 907-917 (2006)

[4] M.G. Coco, S. C. Aro, S. A. McDaniel, A. Hendrickson, J. P. Krug, P. J. Sazio, G. Cook, V. Gopalan, J. V. Badding, “Continuous wave Fe^{2+}:ZnSe mid-IR optical fiber lasers” Optics Express 28 (20), 30263-30274 (2020)

[5] J. Zhao, X. Zheng, E. P. Schartner, P. Ionescu, R. Zhang, T.-L. Nguyen, D. Jin, H. Ebendorff-Heidepriem, “Upconversion Nanocrystals Doped Glass: A New Paradigm for Photonic Materials”, Advanced Optical Materials 4 (10), 1507-1517 (2016)

[6] Y. Ruan, H. Ji, B. C. Johnson, T. Ohshima, A. D. Greentree, B. C. Gibson, T. M. Monro, H. Ebendorff-Heidepriem, “Nanodiamond in tellurite glass Part II: practical nanodiamond-doped fibers”, Optical Materials Express 5 (1), 73-87 (2015)

[7] H. Ebendorff-Heidepriem, T. M. Monro, “Analysis of glass flow during extrusion of optical fiber preforms,” Optical Materials Express 2 (3), 304-320, (2012)

[8] M. J. Chen, Y. M. Stokes, P. Buchak, D. G. Crowdy, H. T. C. Foo, A. Dowler, H. Ebendorff-Heidepriem, “Drawing tubular fibres: experiments versus mathematical modelling”, Optical Materials Express 6 (1), 166-180 (2016)

[9] S. Mochizuki, K. Umezawa, “Optical absorption and photoluminescence of ZnSe microcrystals in a Pyrex glass matrix”, Journal of Physics: Condensed Matter 8 (40), 7509-7521 (1996)

[10] http://www.pmoptics.com/corning_pyrex.html

[11] Schott, https://shop.schott.com/advanced_optics/en/F2/c/glass-F2

[12] T. Mito, H. Takebe, K. Morinaga, “Refractive index and its dispersion of Na_2O-GeO_2 glasses”, Journal of the Ceramic Society of Japan 103 (1201), 886-890 (1995)

[13] H. Li, “Refractive index of ZnS, ZnSe, and ZnTe and its wavelength and temperature derivatives”, Journal of Physical and Chemical Reference Data 13 (1), 103-150 (1984)

[14] https://www.pveducation.org/pvcdrom/materials/znse

[15] X. Pan, J. Zhao, G. Qian, X. Zhang, Y. Ruan, A. Abell, H. Ebendorff-Heidepriem, “Mechanistic insight into the non-hydrolytic sol-gel process of tellurite glass films to attain a high transmission”, RSC Advances 10, 2404-2415 (2020)